

The Local Bubble, Local Fluff, and Heliosphere

Priscilla C. Frisch

University of Chicago, Dept. of Astronomy & Astrophysics, 5640 S. Ellis Ave.,
Chicago, IL 60637

Abstract. The properties of the Local Bubble, Local Fluff complex of nearby interstellar clouds, and the heliosphere are mutually constrained by data and theory. Observations and models of the diffuse radiation field, interstellar ionization, pick-up ion and anomalous cosmic-ray populations, and interstellar dust link the physics of these regions. The differences between the one-asymmetric-superbubble and two-superbubble views of the Local Bubble are discussed.

1 Introduction

The Local Bubble, the Local Fluff complex of nearby interstellar clouds, and the heliosphere, are three astronomical phenomena with properties that can not be determined independently. The Local Bubble (LB) radiation field influences the ionization of both nearby interstellar gas and the heliosphere. The ionizations of nearby interstellar gas and pick-up ions in the heliosphere constrain this radiation field. The kinematics and properties of interstellar gas within and without the heliosphere can be compared to set the confinement pressure of the heliosphere and bow shock, and therefore the interstellar pressure. Interstellar grains observed within the solar system constrain the properties of dust in interstellar clouds. The morphology, properties and kinematics of nearby interstellar gas must be consistent with models of the origin of the soft X-ray background (SXRb).

The LB, Local Fluff and heliosphere make a science “pyramid”, and the interrelation of the physical properties of these three regions is shown in Fig. 1. (The caption to Fig. 1 also summarizes the abbreviations used in this paper.) In this context, the local interstellar matter (LISM) is the same as the “Local Fluff” complex of interstellar clouds (LFC) within about 35 pc of the Sun.

This conference, organized so beautifully by Dieter and his colleagues in Garching, is a timely sequel to two conferences in the last two decades on interstellar gas in the heliosphere, and on the local interstellar medium.¹ The initial linking of the Loop I superbubble, the LISM, and the neutral interstellar gas detected within the solar system was presented in a series of papers culminating

¹ These two conferences were the meetings on “Interstellar Gas in Interplanetary Space, VI. MPAE Lindau Workshop”, June 18–20, 1980, held in Lindau, Germany, and “Local Interstellar Medium, IAU Colloquium No. 81”, held in Madison, Wisconsin June 4–6, 1984.

Welty et al. 1994, Crawford & Dunkin 1995) are nearly equal, although a possible velocity gradient is present in the LFC. At that time, the deceleration of interstellar gas at the heliopause was unknown (c.f. Lallement et al. 1993). The interstellar cloud fragment which surrounds the solar system is a member of the cloud complex seen in front of α Oph and other stars in the galactic center hemisphere of the sky. The enhanced abundances of interstellar refractory elements Ca^+ , Fe^+ and Mn^+ seen in front of α Oph led me to also conclude that the Sun resided in the edge of the Loop I supernova remnant associated with the Scorpius-Centaurus stellar association. The sightline towards α Oph exhibits the strongest interstellar Ca^+ seen towards any nearby star. The need to reconcile the asymmetric distribution of interstellar gas within 30 pc of the Sun (e. g. Frisch 1996, Table 1) and the symmetry of the “bubble” inferred to explain the SXRb led to my suggestion that the Loop I supernova remnant had expanded asymmetrically into the low density interarm region surrounding the solar system. A different model forms the SXRb in an independent supernova explosion around the Sun (unrelated to Loop I) (e. g. Davelaar et al. 1980, Egger, this volume). These contrasting views are reviewed in Breitschwerdt et al. (1996). In this summary I will discuss:

- the heliosphere as a probe of the cloud surrounding the solar system (CSSS) and the Local Bubble (LB)
- the constraints LISM gas places on the LB by shadowing (or lack thereof)
- abundance and kinematical considerations, morphology and structure, and the historical heliosphere.
- My perspective of the LB.

One point needs to be emphasized strongly. There is an underlying question that must be answered, and that question is “What is the Local Bubble?” The region of space commonly referred to as the “Local Bubble” coincides with the interior of Gould’s Belt and with the surrounding interarm region, therefore the answer to this question is not so obvious. Fig. 2 compares the distribution of interstellar clouds within 500 pc to the space motions of the Sun and CSSS. I adopt the view of defining the LB by its walls (Cox & Reynolds 1987). Column densities $N(\text{H}^\circ)$ of $10^{19.8} \text{ cm}^{-2}$ and 10^{20} cm^{-2} attenuate the B and C band radiation, respectively, by a factor of ~ 3 , giving a natural definition for the “walls” of the Local Bubble as the location where $N(\text{H}) \geq 10^{19.8} \text{ cm}^{-2}$, and the ISM opacity in the B-band exceeds unity.

2 The Heliosphere as a Probe of the LISM and LB

By way of background, I will summarize briefly the heliosphere (HS) structure and the properties of the CSSS. The overall structure of the heliosphere appears to be a two-shock structure, with an inner “termination shock” where the solar wind goes from supersonic to subsonic, the heliopause which is the stagnation surface between the solar wind and interstellar plasma components, and

a bow shock surrounding the heliosphere. The CSSS has properties $T \sim 7,000$ K, $n(\text{H}^o) \sim 0.2 \text{ cm}^{-3}$ and $n(\text{p}^+) = n(\text{e}^-) \sim 0.1 \text{ cm}^{-3}$. A magnetic field is present, of unknown strength, but likely to be weak ($B \sim 1.5 \mu\text{G}$, Frisch 1995, Gloeckler et al. 1997). The relative velocity between the Sun and CSSS is $\sim 26 \text{ km s}^{-1}$, approaching from the direction $l \sim 5^\circ$, $b \sim +16^\circ$ in the rest frame of the Sun. In the rest frame of the Local Standard of Rest, this corresponds to a cloud moving towards us at $19\text{--}20 \text{ km s}^{-1}$ from the direction $l \sim 335^\circ$, $b \sim -2^\circ$.⁴ Neutral interstellar atoms cross the heliosphere into the solar system, and turn into the pick-up ion population after ionization (by charge exchange with the solar wind and photoionization) and capture by the solar wind. The pick-up ions are accelerated (perhaps at the termination shock of the solar wind) and create the anomalous cosmic ray population, which propagates throughout the HS.

Heliosphere observations give direct data on the physical properties of the interstellar cloud which surrounds the solar system, the LFC, and radiation field within the LB. Listing the ways in which observations within the heliosphere serve as useful probes of the LISM and LB:

- The CSSS feeds interstellar neutrals into the HS. Thus, observations of pick-up ions and anomalous cosmic rays within the heliosphere provide direct information on the ratios of interstellar neutrals in the CSSS. The pick-up ion (PUI) and anomalous cosmic ray (ACR) data can thus be used to constrain interstellar ionization. Because the ionization levels are sensitive to the radiation field, in turn the PUI and ACR data prove to be a probe of the radiation field within the LB (see Slavin and Frisch, this volume, and Frisch and Slavin 1996). The elements He, Ne, H, O, N, C, and Ar have been observed in either the pick-up ion or anomalous cosmic ray populations. Since C^o is a subordinate ionization state of carbon in the LISM, the C/O ratio in the PUI and ACR populations yield an estimate of the ionization of the CSSS (Frisch 1994).
- Observations of $L\alpha$ and 584 Å backscattered radiation from interstellar H^o and He^o inside of the solar system, respectively, yield information on the temperature, velocity and density of the interstellar cloud which feeds neutrals into the solar system (e.g. Quemerais et al. 1996, Flynn et al. 1997, Adams & Frisch 1977, Scherer et al. 1997).
- Observations of $L\alpha$ absorption from the pile-up of interstellar H^o outside of the heliopause stagnation surface, due to the charge-exchange coupling of interstellar H^o and protons, constrain the fractional ionization of the surrounding cloud and the Mach number of the bow shock of the solar system. The absorption from this pile-up must be included in $L\alpha$ profile fitting for absorption lines in nearby stars, for good D/H ratios. In the α Cen direction, an outer heliosphere model with Mach number=0.9, $n(\text{H}^o)=0.14 \text{ cm}^{-3}$, $n(\text{e}^-)=0.1 \text{ cm}^{-3}$, $T=7600$ K, $V=26 \text{ km s}^{-1}$ yields the best fit, to within

⁴ Note that since the Sun is immersed in this flowing cloud, and the Sun itself moves through space, the solar motion must be removed from the observed upwind direction in order to get the true space velocity of the CSSS in the Local Standard of Rest.

- the limited parameter range considered, to observations of $L\alpha$ absorption towards α Cen (Gayley et al. 1997).
- Interstellar dust observed by Ulysses and Galileo constrain the mass distribution of interstellar dust grains in the CSSS, with a mean mass of 3×10^{-13} gr corresponding to a grain radius of 0.3 cm^{-3} for silicate density 2.5 gr cm^{-3} (Baguhl et al. 1996).

3 LISM Constraints on the Local Bubble and Heliosphere

Models of the conductive interface between the LFC and LB plasmas, when compared to PUI, ACR, and interstellar absorption line data, give direct information on the LB radiation field, LFC conductivity, magnetic field, and other physical quantities (Slavin 1989, Slavin and Frisch, this volume). The morphology, abundance patterns, ionization, density and temperature of the cloud fragments which constitute the Local Fluff cloud complex give direct information on the physical history of the LISM. For instance, the enhanced abundance patterns seen in the LFC, in comparison to abundances seen in cold interstellar clouds, are interpreted as indicating that nearby interstellar material has been processed through a shock front (Frisch 1996). The velocity of the LISM gas indicates an outflow of gas from the Scorpius-Centaurus Association (SCA), suggesting, together with the anomalous abundances, that the LFC is part of the superbubble associated with star formation in this region. The flow of interstellar gas is seen in thirty-six interstellar Ca^+ absorption components seen in 17 nearby stars yield a relatively coherent flow velocity of $-0.1 \pm 2.2 \text{ km s}^{-1}$ in a rest frame defined by the heliocentric velocity vector $l=6^\circ.2$, $b=+11^\circ.7$, $V=-26.8 \text{ km s}^{-1}$ (Frisch 1997a).

The asymmetry of the LISM gas, within about 35 pc, belies the symmetry inferred for the local component of the SXR. Table 1 illustrates this well known property. This asymmetry, and the fact that clouds in the LFC flow outwards from the SCA, must be explained by any theory on the origin of the Local Bubble. Note that because of this asymmetry, most of the mass within 35 pc is in the galactic center hemisphere of the sky.

One important question: Can the LFC shadow the 0.25 keV SXR and thereby give us information on the spatial distribution of the emitting plasma? Typical column densities to the “edge” of the LFC in several directions are given in Table 1, where the edge distance is defined as $N(\text{H}^\circ)/0.20$. The column densities are estimates in some cases, based on $N(\text{Ca}^+)/N(\text{H}^\circ)=10^8$, and an average cloud space density of 0.20 cm^{-3} is used. From this, it can be seen that most of the interstellar gas in the LFC cloud complex has column densities too low to provide significant shadowing of the SXR – i. e. well below the $10^{19.8} \text{ cm}^{-2}$ value needed to shadow the B-band. The exceptions are the α Oph ($l=36^\circ$, $b=+23^\circ$, $d=14 \text{ pc}$) and HD149499B ($l=330^\circ$, $b=-7^\circ$, $d=37 \text{ pc}$) sightlines, with column densities $\log N(\text{H}^\circ) \sim 19.57$, $\sim 19.00 \text{ cm}^{-2}$, respectively. The α Oph column density is not well known. In these directions 10% – 50% percent attenuation of

Table 1. Column Densities through Local Fluff

l,b(deg)	log N(H) ^a	d(pc) ^b	l,b(deg)	log N(H) ^a	d(pc) ^b
28,+15	18.86	10	240,-11	17.9	1.1
101,65	17.85	1.0	289,-54	18.90	1.1
163,+5	18.24	2.7	295,+46	18.53	4.8
214,+13	17.88	1.1	330,-7	19.00	14
214,-60	18.70	0.7	350,-53	18.49	4.4

^a Log N(H)=log N(H^o+H⁺). See Frisch & Welty 1997, Frisch 1997b, Napiwotzki et al. 1995 for original references. ^bd(pc) is the distance to the LFC edge, which is calculated for n(H^o)=0.20 cm⁻³.

the B-band emission may be expected. These stars are in the direction of the dominant shadow (due to H^o filaments composing the Loop I shell, Cleary et al. 1979) in front of the X-ray emission from Loop I. The star HD149499B is located within $\sim 10^\circ$ of the LFC flow direction in the Local Standard of Rest. Hardening of the SXRb is expected, in agreement with the observations of a dipole gradient pointed towards l=168^o.7, b=11^o.2 (Snowden et al. 1990). The plasma emitting in the 0.10–0.18 keV region in the upwind hemisphere must be in front of the nearest 6×10^{19} cm⁻² hydrogen column density. This plasma could, therefore, be behind the upwind cloud with no significant shadowing. Alternatively, the prevalence of very small structure in the ISM allows the possibility that the plasma and cooler clouds forming the LFC are interspersed.

4 Journey of the Sun through Space

Our improved understanding of the morphology and kinematics of nearby ISM in comparison to the space trajectory of the Sun permit a deeper understanding of the historical changes in the galactic environment of the Sun, and the effect those changes have on the heliosphere. From Fig. 2, we see that within the past $\sim 100,000$ –200,000 years the Sun emerged from the void of the surrounding interarm region and entered the LF complex of clouds. Within the past 10,000 years, and perhaps within the past 2,000 years, the Sun appears to have entered the cloud in which it is currently situated (Frisch 1997a). The physical properties of these clouds constrain the configuration and properties of the heliosphere. It is notable that the space velocities of the Sun and CSSS are nearly perpendicular, so that these ages are highly sensitive to uncertain assumptions about cloud morphology and kinematics.

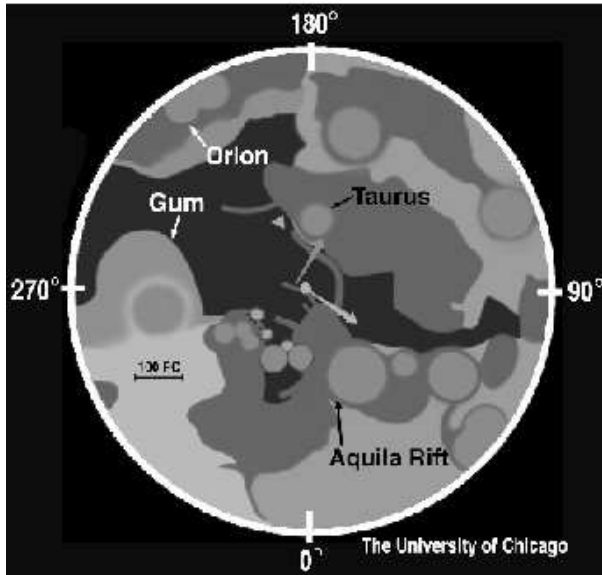


Fig. 2. The distribution of interstellar molecular clouds (traced by the CO 1- \rightarrow 0 115 GHz rotational transition, Dame and Thaddeus 1985) and diffuse gas (traced by E(B-V) color excess due to the reddening of starlight by interstellar dust Lucke 1978) within 500 pc of the Sun are shown. The round circles are molecular clouds, and the shaded material is diffuse gas. Interstellar matter is shown projected onto the galactic plane, and the plot is labeled with galactic longitudes. The distribution of nearby interstellar matter is associated with the local galactic feature known as “Gould’s Belt”, which is tilted by about 15–20° with respect to the galactic plane. Thus, the ISM towards Orion is over 15° below the plane, while the Scorpius-Centaurus material (longitudes 300°–0°) is about 15–20° above the plane. Also illustrated are the space motions of the Sun and local interstellar gas, which are nearly perpendicular in the LSR velocity frame. The three asterisks are three subgroups of the Scorpius-Centaurus Association. The three-sided star is the Geminga Pulsar. The arc towards Orion represents the Orion’s Cloak supernova remnant shell. The other arcs are illustrative of superbubble shells from star formation in the Scorpius-Centaurus Association subgroups. The smallest (i. e. greatest curvature) shell feature represents the Loop I supernova remnant.

5 Origin of the Local Bubble—One vrs. Two Bubbles

What is the Local Bubble? There is no agreement on the answer to this question. Ask an X-ray astronomer and they will probably tell you that it is the physical location of the 10^6 K plasma from a recent local supernova explosion that emits radiation in the 0.1–0.18 KeV B-Band and 0.25 keV C-Band. Ask a radio astronomer, and they may be confused because the Sun is located in an interarm region between the Orion spiral arm and the Local Arm, which is a short (~ 1 kpc long) spur projecting from the Orion Arm. Spiral arms are traced out by strings of molecular clouds and star-forming regions, and Fig. 2 illustrates the nearby molecular clouds as defined by observation of CO. Interarm regions are

regions with very low densities of interstellar matter.

Historically, the LB concept is a mixture of the view that a separate local supernova explosion formed the SXR_B (e. g. Davelaar et al. 1980, Cox & Reynolds 1987) and the view that the superbubble formed by the successive epochs of star formation in the Scorpius-Centaurus Association have expanded asymmetrically into the low density interarm region surrounding the Sun (Frisch 1981, Frisch 1995). The Davelaar et al. view has been updated by Egger and Aschenbach (1995, EA, also Egger, this volume), who attribute the conventional H⁰ filaments which bound the Loop I supershell, and which are threaded by a displaced galactic magnetic field, to a collision between the supernova around the solar system and the Loop I superbubble.

The salient properties of the asymmetric superbubble model for the LB are (see Frisch, 1995, for more details):

- The three epochs of star formation (4–15 Myrs ago) in the SCA each created superbubble structures, with the later structures evolving within the cavities formed by the earlier events. In the asymmetric superbubble view these shells will have expanded asymmetrically into the low density interarm region surrounding the Sun. The ISM surrounding the superbubbles was initially asymmetric because of the local arm–interarm configuration, and the Aquila Rift molecular cloud between $l \sim 20^\circ$ and $l \sim 40^\circ$.
- The Loop I supernova remnant, $\sim 250,000$ years old (Borken & Iwan 1977), is confined because it expanded into, and ablated material from, the Aquila Rift molecular cloud. This can be seen in the galactic interval $l = 17^\circ - 27^\circ$, $b = 0^\circ - 10^\circ$ when the configuration of the Aquila Rift CO cloud (Dame and Thaddeus 1985) is compared with the narrow neck region of the North Polar Spur (Sofue and Reich 1979). The Aquila Rift molecular cloud is the node region where all of the superbubble shells from the three epochs of star formation in the SCA, as well as the most recent supernova explosion creating the North Polar Spur, converged after plowing into the molecular gas and decelerating. I propose here that the soft X-ray emission associated with the North Polar Spur itself occurs in a position consistent with the formation of a galactic fountain with a footprint in the disrupted Aquila Rift molecular cloud.
- The characteristic filamentary structure seen in the H⁰ gas, which defines the annular ring attributed to the merged bubbles, appears to be due to confinement by the $\sim 5 \mu\text{G}$ magnetic field embedded in the filaments (Cleary et al. 1979) and does not require the explanation of merging bubbles. The superbubble shell boundaries portrayed in Fig. 2 represent the 21 cm filaments which are seen at negative galactic latitudes between $l \sim 40^\circ$ and $l \sim 180^\circ$, and which are threaded by the ambient magnetic field as is seen by Zeeman splitting and stellar polarization measurements.
- The LFC is part of the expanding superbubble shell from the formation of the Upper Scorpius subgroup 4–5 Myrs ago. Towards larger galactic latitudes, $l = 350^\circ$ to $l = 40^\circ$, corresponding to the eastern boundary of Loop I,

the expansion of the shells was impeded by collision with the Aquila Rift molecular gas. At lower longitudes, or the western boundary of the Loop I superbubble, expansion proceeded more freely and earlier shells expanded past the solar location, reheating the low density gas in the anti-center interarm region.

- The Loop I supernova remnant has expanded inside of the Upper Scorpius subgroup superbubble, and encountered denser ambient gas than did the previous superbubble shells because of the proximity to the denser Aquila Cloud. The upwind direction in the Local Standard of Rest, $l \sim 335^\circ$, $b \sim -2^\circ$, represents a direction offset from the center of the Loop I supernova remnant by about 20° .

The main source of disagreement between the asymmetric-superbubble versus symmetric-superbubble views is the requirement that in the latter scenario, a separate supernova explosion in the anti-center hemisphere explains the SXR. In the former view, the source of the SXR is the ambient plasma inside of the superbubble shells formed by the first star formation epochs in the SCA reheated by unspecified shocks and energetic radiation that would propagate freely through the very low density material. In the two-bubble scenario, a coherent dense wall of neutral hydrogen at 40–70 pc, with $N(\text{H}^0) \sim 10^{20} \text{ cm}^{-2}$ is postulated to separate the two bubbles, but there is no observational evidence for such a wall within 50 pc covering the central regions of the Loop I bubble. Counter-examples are easily found. For example, comparing the stars β Cen ($l=312^\circ$, $b=1^\circ$, $d=161$ pc, $\log N(\text{H}^0) \leq 19.5 \text{ cm}^{-2}$, Fruscione et al. 1994), and HD 149499 B ($l=330^\circ$, $b=-7^\circ$, $d=37$ pc, $\log N(\text{H}^0)=19.0 \text{ cm}^{-2}$) show that over 30% of the nearby gas is associated with the LFC. The absence of X-ray emission from the Loop I interior may be due to the fact this is an evacuated cavity. An adequate model for the SXR emission mechanism is required to establish its origin (Sanders, this volume) and help resolve these differences.

The two scenarios agree on the distance of the H^0 21 cm filaments, which are established by reddening measurements. The LFC is in the interior of the ring, but it has distance <40 pc. I believe the LFC is gas which is part of an expanding superbubble shell from the SCA.

This research has been supported by NASA grant NAGW-5061.

References

- Adams, T. F., & Frisch, P. C. 1977, ApJ 212, 300
 Baguhl, M., Grun, E., and Landgraf, M. 1996, Space Science Reviews 78, 165
 Borken, R. J., & Iwan, D. C. 1977, ApJ, 218, 511
 Cleary, M. N., Heiles, C., & Haslam, C. G. T. 1979, AAS, 36, 95.
 Breitschwerdt, D., Egger, R., Freyberg, M. J., Frisch, P. C., & Vallergera, J. V. 1996, Space Science Reviews 78, 183
 Cox, D. P., & Reynolds, R. J. 1987, ARAA 25, 303
 Crawford, I. A. & Dunkin, S. K. 1995, MNRAS 273, 219

- Dame, T. M., Thaddeus, P. 1985, *ApJ* 297, 751
Davelaar, J., Bleeker, J. A. M., & Deerenberg, A. J. M. 1980, *AA* 92, 231
Egger, R. J. & Aschenbach, B. 1995, *AA* 294, L25.
Flynn, B., J., Vallerga, J., Dalaudier, F., and Gladstone, G. R. 1997, submitted to *J. Geophys. Res.*
Frisch, P. C. 1981, *Nature* 293, 377
Frisch, P. C. 1994, *Science* 265, 1423
Frisch, P. C. 1995, *Space Science Reviews* 72, 499
Frisch, P. C. 1996, *Space Science Reviews* 78, 213
Frisch, P. C. 1997a, submitted to *Science*
Frisch, P. C. 1997b, *Proceedings of ACE Workshop*, in press
Frisch, P. C., & Slavin, J. D. 1996, *Space Science Reviews* 78, 223
Frisch, P. C. & Welty, D. E. 1997, in preparation
Fruscione, A., Hawkins, I., Jelinsky, P., Wiercigroch, A. 1994, *ApJS*, 94, 127.
Gayley, K. G., Zank, G. P., Pauls, H. L., Frisch, P. C., & Welty, D. E. 1997, *ApJ*, 487, 259
Gloeckler, G., Fisk, L. A., and Geiss, J. 1997, *Nature*, 386, 374.
Lallement, R., Bertaux, J.-L., & Clarke, J. T. 1993, *Science* 260, 1095
Lucke, P. B. 1978, *AA*, 64, 367.
Napiwotzki, R., Hurwitz, M., Jordan, S., Bowyer, S., Koester, D., Weidemann, V., Lampton, M., & Edelstein, J. 1995, *AA* 300, 300
Scherer, H., Fahr, H. J., and Clarke, J. T. 1997, *AA*, in press
Snowden, S. L., Schmitt, J. H., Edwards, B. C. 1990, *ApJ* 364, 118
Quemerais, E., Bertaux, J.-L., Sandel, B. R., & Lallement, R. 1996, *AA* 308, 279
Slavin, J. D. 1989, *ApJ* 392, 718
Sofue, Y., Reich, W. 1979, *AASS* 38, 251
Welty, D. E., Hobbs, L. M., & Kulkarni, V. P. (1994): *ApJ* 436, 152